water

MDPI

Article

Development of a Multiple-Drought Index for Comprehensive Drought Risk Assessment Using a Dynamic Naive Bayesian Classifier

Hyeok Kim [1], Dong-Hyeok Park [2], Jae-Hyun Ahn [3] and Tae-Woong Kim [4,*]

[1] Department of Smart City Engineering, Hanyang University, Seoul 04763, Korea; k4082560@hanyang.ac.kr
[2] RAON Technology & Consulting, Anyang 14116, Korea; smilehyuki@naver.com
[3] Department of Civil Engineering, Seokyeong University, Seoul 02713, Korea; wrr21@naver.com
[4] Department of Civil and Environmental Engineering, Hanyang University (ERICA), Ansan 15588, Korea
* Correspondence: twkim72@hanyang.ac.kr

Abstract: Korea has made various efforts to reduce drought damage; however, socio-economic damage has increased in recent years due to climate change, which has led to increasing frequency and intensity of drought. In South Korea, because precipitation is concentrated in the summer, drought damage will be significant in the event of failure of water resources management. Seasonal and regional imbalances in precipitation have contributed to recent extreme droughts in South Korea. In addition, population growth and urbanization have led to increased water use and contributed to water shortage. Drought risk analysis must address multiple contributing factors and comprehensively assess the effects or occurrence of future droughts, which are essential for planning drought mitigation to cope with actual droughts. Drought mitigation depends on the water supply capacity during dry spells. In this study, a dynamic naive Bayesian classifier-based multiple drought index (DNBC-MDI) was developed by combining the strengths of conventional drought indices and water supply capacity. The DNBC-MDI was applied to a bivariate drought frequency analysis to evaluate hydrologic risk of extreme droughts. In addition, future changes of the risk were investigated according to climate change scenarios. As a result, the drought risk had a decreasing trend from the historic period of 1974–2016 to the future period of 2017–2070, then had an increasing trend in the period of 2071–2099.

Keywords: dynamic naive Bayesian classifier; multiple drought index; hydrologic risk; climate change

Citation: Kim, H.; Park, D.-H.; Ahn, J.-H.; Kim, T.-W. Development of a Multiple-Drought Index for Comprehensive Drought Risk Assessment Using a Dynamic Naive Bayesian Classifier. *Water* **2022**, *14*, 1516. https://doi.org/10.3390/w14091516

Academic Editor: Maria Mimikou

Received: 17 March 2022
Accepted: 5 May 2022
Published: 9 May 2022

1. Introduction

Based on a variety of climate change scenarios, general circulation models (GCMs) predict that global temperature will rise 0.64 °C to 0.70 °C by 2030 compared with 1980. The frequency and intensity of extreme rainfall events and extreme droughts are also expected to increase in many areas, along with heatwaves [1–4]. Research works on Korea's climate predict that the frequency and intensity of droughts will increase [5–7]. When drought occurs, it generally affects a broad region for seasons or years at a time. The proportion of population affected by drought tends to be larger than with other disasters [8]. However, an effective response is possible, because droughts are usually a prolonged and slow-moving disaster.

The drought that occurred in Chungcheong, South Korea during 2014 and 2015 resulted in a continuous drop of water stored in reservoirs by 25.5%, which was a historic record. After the drought of 2014–2015, the need for comprehensive risk assessment and effective response measures of extreme drought is increasing. Drought can cause significant damage to agricultural production and economies; nevertheless, in general, the absence of a unique definition of drought makes it difficult to know when and where drought occurs. There is also no recognized universal drought index [9], although conventional indices have been developed for use in monitoring meteorological, agricultural, and hydrological drought [10–12]. More recently developed indices can comprehensively determine and evaluate drought severity [9]. To develop a multiple drought index, this study attempts to combine the standardized precipitation index (SPI), streamflow drought index (SDI), evaporative stress index (ESI), and waters supply capacity index (WSCI). Generally, droughts are classified into four different types, i.e., meteorological, hydrological, agricultural, and socioeconomic drought. A multiple drought index that combines several drought indices can accurately represent drought characteristics, because drought occurs from interconnected factors [13]. Thus, many researchers have developed multiple indices that compose pre-developed indices [14–16].

We used a dynamic naive Bayesian classifier (DNBC) to calculate a multiple-drought index. The DNBC that has been used for probabilistic univariate drought prediction and assessment recently is an extension of Hidden Markov Model (HMM) [17,18]. When the amount of training samples is limited, the DNBC has the advantages of reducing the number of model parameters, improving training time, and performing better than HMM [14,19]. Various efforts have been made to apply Bayesian theory to drought assessment. Shin et al. [20] used a Bayesian network model to produce probabilistic predictions of hydrological drought. Yoo et al. [21] used a Bayesian network to probabilistically assess the sensitivity of the meteorological drought index. Most notably, Chen et al. [14] incorporated multiple drought indices, such as SPI, SDI, and a normalized vegetation supply index (NVSWI), in a comprehensive drought evaluation, then adopted and analyzed the DNBC for probabilistic drought evaluation and evaluated droughts to a degree of accuracy greater than that of any single index. Even though various indices are developed and employed according to the respective goals, the drought characteristics vary from region to region, and drought impacts may not be realized in agriculture and human society, even if meteorological drought progresses. In addition, if water resources are concerned, different types of drought make it difficult to assess and manage drought effectively. In this study, we used the DNBC to assess and evaluate drought severity considering its various causes, including regional water supply capacity, which significantly affects regional drought response capacity.

Other attempts have been made to assess the risk of drought using a bivariate drought frequency analysis (BDFA). Previous analyses of variations on rainfall deficiency and the standard precipitation index have led to more attempts to calculate drought risk. Yoo et al. [22] conducted frequency analysis using the copula function to combine drought severity and duration and quantified uncertainty in frequency analysis results. Yu et al. [23] used dam inflow data to define hydrological drought and performed the BDFA to evaluate water supply capacity. Chen et al. [24] and Mirabbasi et al. [25] conducted the BDFA by applying a copula function to drought severity and duration. Kim et al. [26] applied Bayesian analysis to a copula model to assess the uncertainty of the parameter. Yu et al. [27] estimated a joint probability distribution function of drought duration and severity and calculated hydrologic risks for critical drought events. In this study, we performed the BDFA using a DNBC-MDI to estimate drought return periods and assessed drought risk in a region. Drought risk can be used as a reference in drought planning and mitigation.

2. Overview of Method and Data

We developed a practical method of calculating drought risk combining various drought indices and evaluating changes in risk according to climate change scenarios. According to Chen et al. [14] and Mallya et al. [17], probabilistic assessment of drought using several factors produced better results than using conventional droughts indices.

The first step was to calculate individual drought indices using observed and synthetic data. We used observed data from 1974 to 2016 and synthetic data from 2017 to 2099 generated by the HadGEM2-AO, which is one of the representative global models used by the Korea Meteorological Administration (KMA) to calculate climate change scenarios through the standard experimental system of Coupled Model Intercomparison Project phase 5, under the Intergovernmental Panel on Climate Change (IPCC) representative concentration pathway (RCP) 8.5 scenario. In this study, using observed and synthetic data, the SPI, SDI, ESI, and WSCI were calculated and used as the inputs to the DNBC.

The second step was to calculate a multiple drought index. Drought is usually defined as a natural disaster caused by a lack of precipitation. However, damage from drought occurs if sufficient water is not secured reliably enough to meet the demand of water users. If water is secured reliably, there is no damage, even during a prolonged drought. To calculate the drought risk, a drought index must, therefore, consider the water supply capacity. In this study, the WSCI was employed to represent the water supply capacity, which was developed by Lee et al. [28] to assess how long a reservoir can meet the demand for water. Taking inspiration from Chen et al. [14], who applied the DNBC to combine the SPI, SDI, and NVSWI, we calculated a DNBC-based multiple drought index (DNBC-MDI) combining the SPI, SDI, ESI, and WSCI. The DNBC-MDI was expected to represent actual drought areas by incorporating the effects of water supply capacity with other drought indices. In addition, using the DNBC-MDI, we can compare and assess the current drought risk posed to South Korea from climate change.

The third step was to analyze current and future drought risks based on drought return periods after performing the BDFA of the DNBC-MDI. Yu et al. [27] demonstrated that the BDFA was useful for calculating hydrological drought risk, because return periods of drought were easily determined from the BDFA. Determining drought risk using the DNBC-MDI allowed for assessing how the risk varies with water supply capacity. Figure 1 is a flow chart of this study.

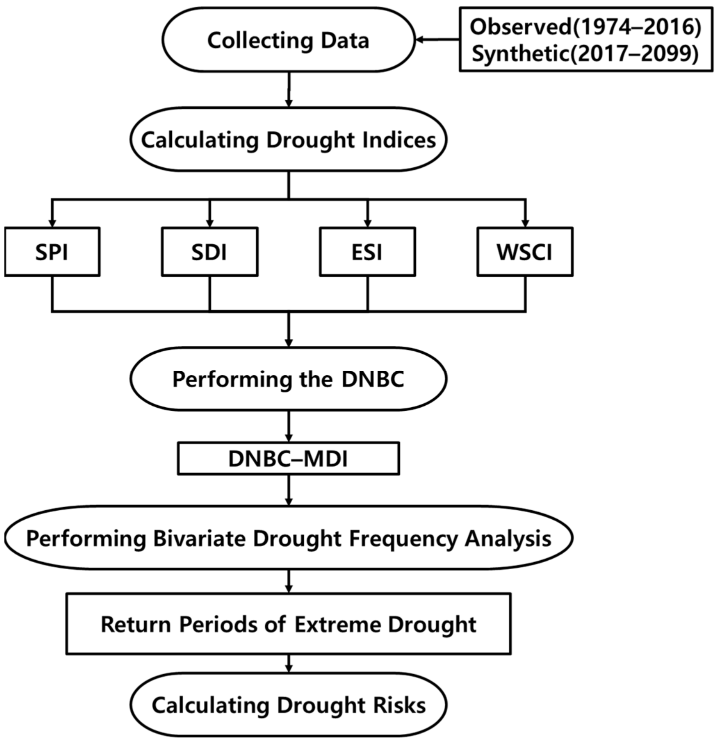

Figure 1. Flow chart of the study.

The study is in the Han River basin, located at 36°48′–38°55′ north latitude and 125°69′–129°29′ east longitude. It is the largest basin in Korea and accounts for 25 percent of the country's area. The average monthly temperature is 23–25 °C in summer and −6–3 °C in winter, and the average precipitation in summer is 1272.5 mm, accounting for 70% of the average annual precipitation.

We collected, observed, and synthesized data from the KMA website (http://www.kma.go.kr (accessed on 27 March 2020)), Water Resources Management Information System (http://www.wamis.go.kr (accessed on 22 February 2020)), and Asia-Pacific Economic Cooperation Climate Center (https://www.apcc21.org (accessed on 13 June 2021)) for 26 sub-basins in the Han River basin, excluding North Korea portions, as shown in Figure 2. To compare variations according to the climate change scenario, the periods were divided into P-0 (1974–2016), P-1 (2017–2040), P-2 (2041–2070), and P-3 (2071–2099).

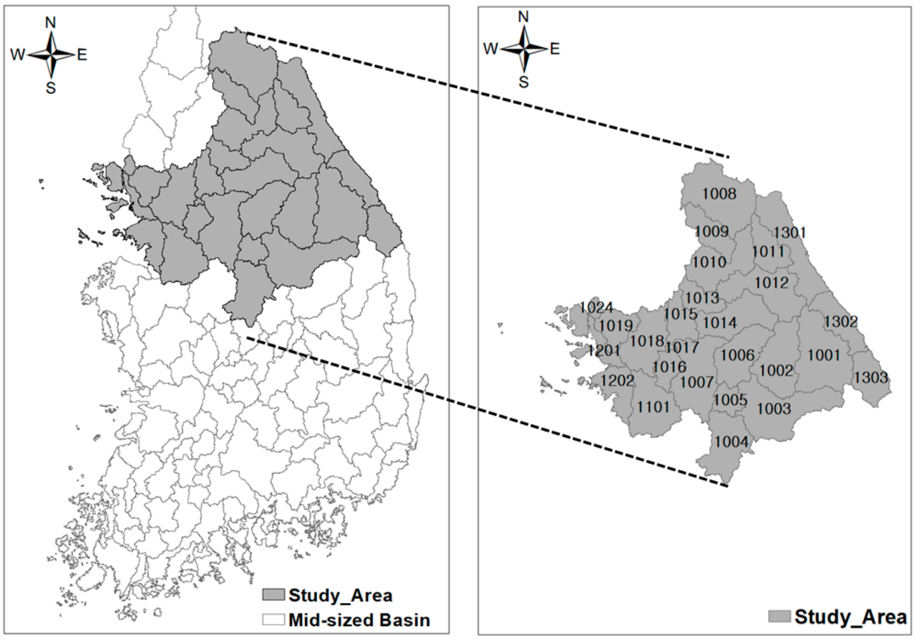

Figure 2. Study area (The four-digit number in the right panel indicates the sub-basin ID code).

3. Dynamic Naive Bayesian Classifier (DNBC)

The DNBC is a simple probabilistic classifier based on Bayes' theorem with strong naive assumptions of conditional independence among the attributes given the hidden state. The model is composed of a set $A = \{A_t \mid t = 1, \ldots, T\}$, where each $A_t = \{A_t^n \mid 1 \le n \le N\}$ is a set of N attributes generated by the dynamic process at state $S_t = \{1, \ldots, m\}$ [15]. A_t^n identifies a specific attribute, e.g., an individual drought index, while S_t denotes a realization of the drought state with different severity at time t. The joint likelihood of observed attributes and latent states in a DNBC can be expressed by Equation (1).

$$P(A_{1:T}, S_{1:T}) = P(S_1) \prod_{t=1}^{T-1} P(S_{t+1}|S_t) \prod_{t=1}^{T} \prod_{n=1}^{N} P(A_t^n|S_t) \tag{1}$$

where $P(S_1)$ is the initial probability distribution for the hidden state S_t at time $t = 1$; $P(S_{t+1}|S_t)$ is the transition probability from S_t to S_{t+1}; and $P(A_t|S_t) = \prod_{n=1}^{N} P(A_t^n \mid S_t)$ is the emission probability distribution of an observed attribute at time t given S_t. $P(A_t|S_t) = \prod_{n=1}^{N} P(A_t^n \mid S_t)$ is valid for its naive conditional independence assumption among the attributes given the class. The DNBC follows two main assumptions. The dynamic process of S_t follows the first-order Markov chain property, i.e., the next state is dependent only on the current state. The dynamic process is stationary, i.e., the transition probability is not time-dependent.

We estimated the parameters of the DNBC using the R package "depmixS4" based on the expectation-maximization algorithm, which iteratively maximizes the expected joint log-likelihood of the parameters given the attribute observations and states. In the DNBC, the complete set of parameters for a given model was defined as $\theta = (\theta_1, \theta_2, \theta_3)$ with three vectors demonstrating the parameters for the initial, transition, and emission probabilities, respectively. The joint log-likelihood can be written as Equation (2).

$$\log P(A_{1:T},\ S_{1:T}|\ \theta) = \log P(S_1\,|\theta_1) + \sum_{t=1}^{T-1} \log P(S_t\,|S_{t+1}\,,\theta_2) + \sum_{t=1}^{T} \log P(A_t|S_t,\ \theta_3) \quad (2)$$

In this study, the previously calculated drought indices SPI, SDI, ESI, and WSCI were adopted as input attributes to the DNBC. Assuming that the inputs were independent of each other, we chose a Gaussian distribution for the emission distribution of each attribute, given by Equation (3).

$$P(A_t^n\,|S_t = i) = N\left(A_t^n\,|\mu_i^n\,,\ \sigma_i^{2n}\right),\ n = 1,\ \cdots,\ N,\ i = 1,\ \cdots,\ m \quad (3)$$

where μ_i^N and σ_i^{2n} are the mean and the variance of the Gaussian emission distribution for the ith latent state and the nth observed variable. Chen et al. [14] selected the Gaussian distribution due to its easy computation and availability to account for the drought-related indicator's complex process. With the estimated optimal DNBC parameters, the most probable path of the latent drought state that maximizes $P(A|\cdot)$, together with the probability of each state at every time step, can be obtained using the Viterbi algorithm [14].

4. Results

4.1. Individual Drought Indices

The SPI, SDI, ESI, and WSCI were calculated using the observed and synthetic data to account for the various causes of drought. Figure 3 shows their time series for Chungju Dam basin (# 1005), as a representative example, in which the SPI and SDI showed similar patterns, while the ESI and WSCI showed greater regional variations than seasonal effects. The drought state was classified into seven conditions as shown in Table 1. The average ratio of drought states for all 26 sub-basins is different as follows. Based on the SPI, "Normal" condition was the most common at 66.73 to 70.27%; "Extreme Wet" was 2.27 to 3.40%; and "Extreme Dry" was found to be the least likely to occur at 1.47 to 2.47%. Based on the SDI, "Normal" was the most common at 67.13 to 69.40%; "Extreme Wet" presented 1.40 to 2.93%; and "Extreme Dry" was found to be the least likely at 1.67 to 3.13%. Based on the ESI, "Normal" was the most common at 74.67 to 84.53%; the probability of "Extreme Wet" was almost nonexistent; and "Extreme Dry" presented 4.73 to 6.67%. Based on the WSCI, "Normal" was the highest at 67.13 to 80.93%; "Severe Dry" ranged from 0.73% to 8.40%; and "Extreme Dry" was the least likely to occur at 0.0 to 3.0%.

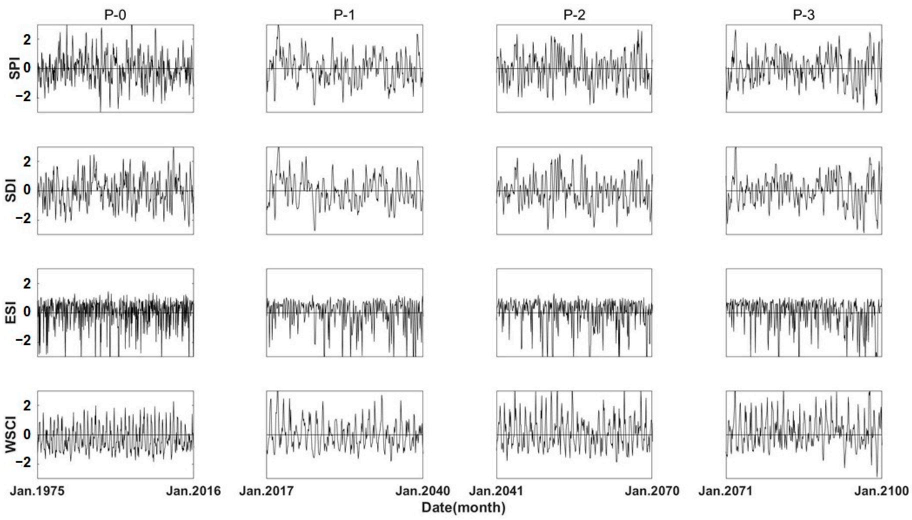

Figure 3. Time series of the SPI, SDI, ESI, and WSCI for Chungju Dam basin (# 1005).

Table 1. Drought indices and moisture conditions.

SPI, SDI, ESI, WSCI	DNBC-MDI	Moisture Condition
2.00~∞	1	Extremely wet
1.50~1.99	2	Very wet
1.00~1.49	3	Moderately wet
−0.99~0.99	4	Normal
−1.00~−1.49	5	Moderately dry
−1.50~−1.99	6	Severe dry
−2.00~−∞	7	Extremely dry

4.2. DNBC-MDI

The DNBC-MDI was calculated by applying the DNBC to drought indices, assuming no association between the input indices. In this study, we assumed that the SPI, SDI, ESI, and WSCI were independent of each other. As shown in Table 1, the DNBC-MDI presents seven drought states, and the sum of the occurrence probabilities corresponding to seven states is 1.

Figure 4 shows the probability of the DNBC-MDI drought states that can occur monthly for Chungju Dam basin (# 1005), as a representative example, in which the larger the color bar of each state, the higher the probability of occurrence of that state. As shown in Figure 4, the probabilities of "Extremely Dry" (yellow bar) were similar for P-1 and P-2 but decreased for P-3 by 0.8%. The probabilities of "Very Wet" tended to extremely decrease for P-1. The probabilities of "Moderately Wet" and "Severe Dry" tended to increase for P-1 and P-2, then decrease for P-3. The probabilities of "Normal" and "Extremely Wet" tended to decrease for P-1, then increase for P-2 and P-3. The probabilities of "Moderately Dry" tended to increase for P-1, P-2, and P-3.

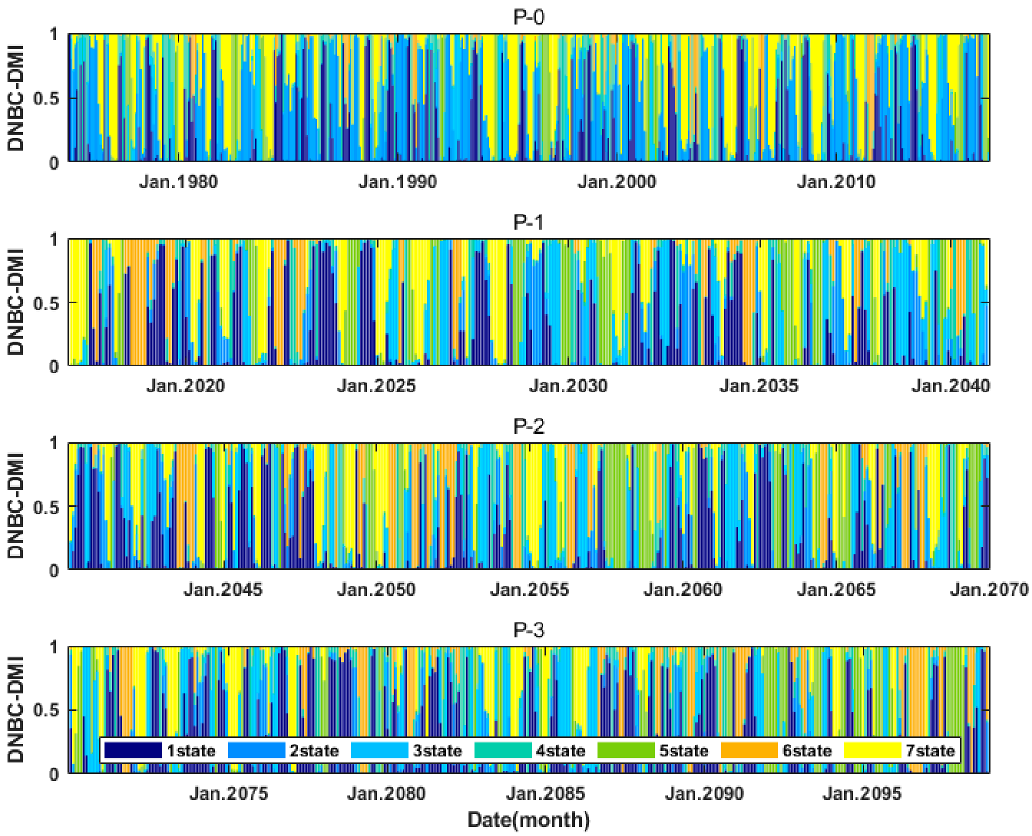

Figure 4. The DNBC-MDI for Chungju Dam basin (# 1005).

4.3. Bivariate Drought Frequency Analysis Using a Copula Function

In this study, a Clayton copula function of the Archimedean family was used for the BDFA after comparing with other copula functions. It is suitable for hydrological analysis, as the Archimedean copula can better reflect the relationship between hydrological variables than the elliptical copula [27,29,30]. Moreover, a Clayton copula function is suitable for drought simulations to reflect the tail structure of the data [31].

The BDFA was performed for 26 sub-basins after extracting drought duration and severity from the time series of DNBC-MDI with threshold of five to seven states. Figure 5 shows the drought severity–duration–frequency curve for Chungju Dam basin (# 1005), as a representative example.

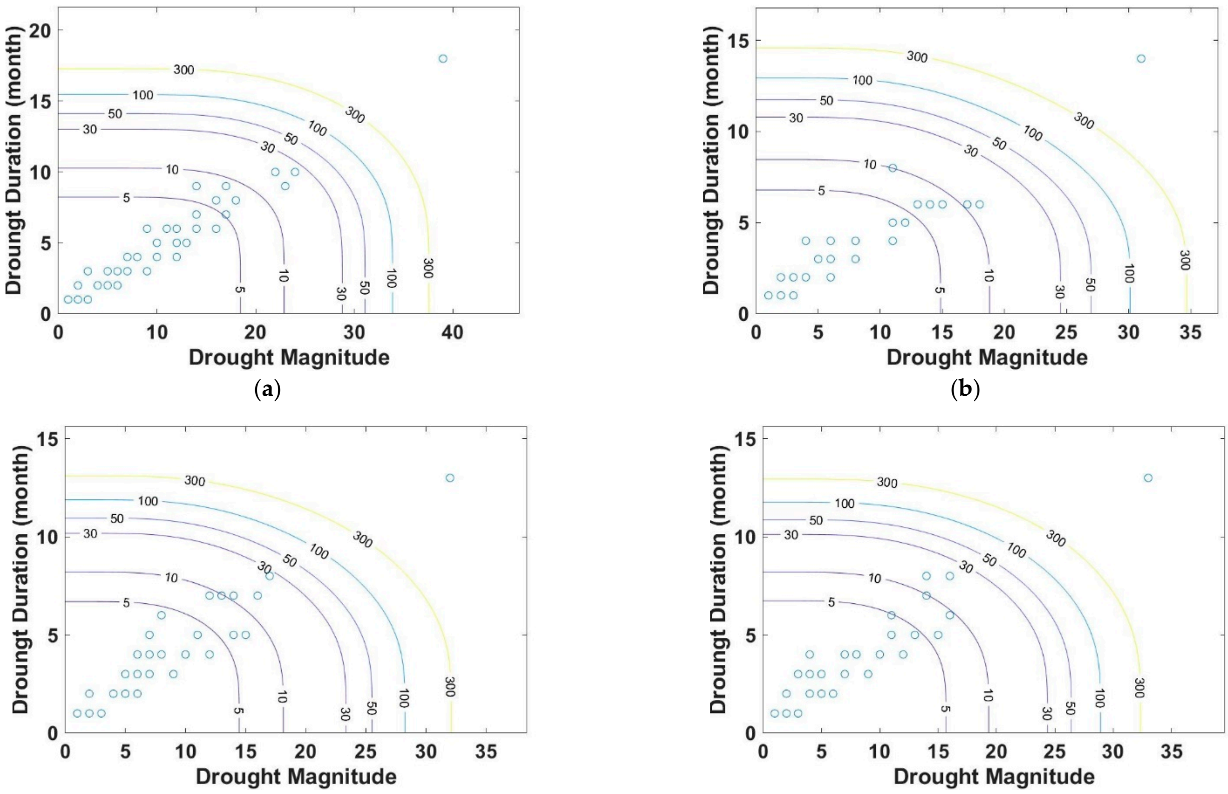

Figure 5. Drought severity–duration–frequency curves for Chungju Dam basin (# 1005). (The circles mean the drought events.) (**a**) P-0(1974–2016); (**b**) P-1(2017–2040); (**c**) P-2(2041–2070); (**d**) P-3(2071–2099).

4.4. Risk Analysis

In this study, drought risk was calculated based on the hydrologic risk in Equation (4), which means the probability that return period T_{ds} will occur for n years. Therefore, a region with a drought risk closer to one is most drought-prone.

$$R = 1 - \left(1 - \frac{1}{T_{ds}}\right)^{n} \tag{4}$$

Using the drought severity–duration–frequency curves in Section 4.3, the maximum return periods were estimated for each sub-basin and period, and the drought risks were calculated for 100 years (n = 100). Figure 6 shows the drought risk using the DNBC-MDI. Sub-basins # 1302 (R = 0.999) and # 1011 (R = 0.999) presented the highest risk during 1974–2016, and # 1005 (R = 0.999) and # 1016 (R = 0.999) were the most dangerous areas during 2017–2040. Sub-basin # 1303 (R = 1.000) and # 1004 (R = 0.999) were at high risk during 2041–2071. Sub-basins # 1301 (R = 1.000) and # 1303 (R = 1.000) were the most dangerous areas in 2071–2099. During 1974–2016, sub-basin # 1303 (R = 0.000) and # 1101 (R = 0.080) were at the lowest risk, while, during 2017–2040, sub-basin # 1019 (R = 0.000) and # 1004 (R = 0.000) were at the lowest risk. During 2041–2070, sub-basin # 1006 (R = 0.100) and # 1016 (R = 0.232) were at the lowest risk, and sub-basins # 1019 (R = 0.000) and # 1014 (R = 0.000) were at the lowest risk during 2071–1999. On average, sub-basins # 1005 and # 1008 were the most dangerous areas, while sub-basins # 1017 and # 1019 were the least dangerous. Drought risk varied over time, but drought risk in the Han River basin was the highest during 1974–2016 at 0.709, while the drought risk during 2041–2070 was the lowest at 0.573. The drought risk in the Han River basin decreased by 2070 but then increased.

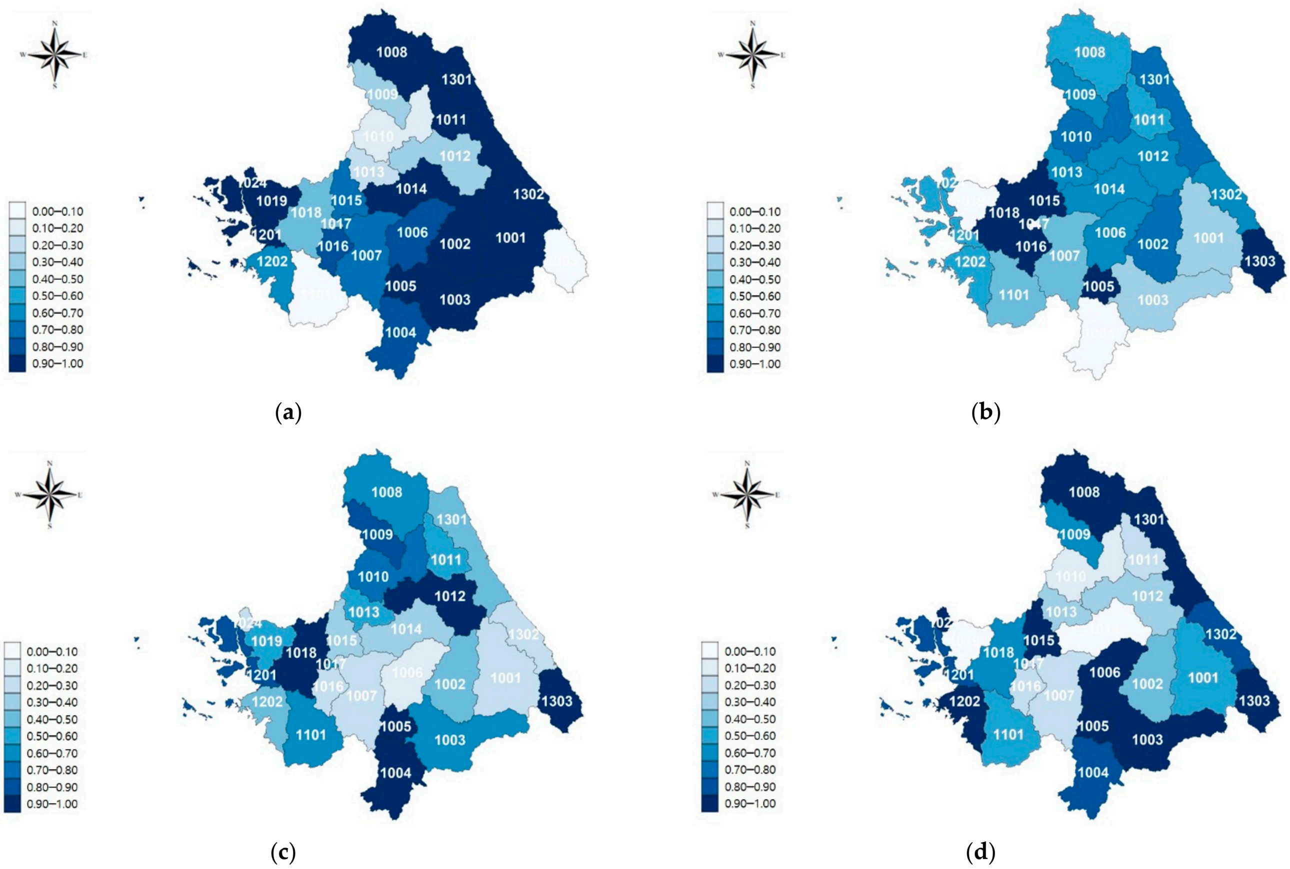

Figure 6. Drought risk using the DNBC-MDI. (**a**) P-0(1974–2016); (**b**) P-1(2017–2040); (**c**) P-2(2041–2070); (**d**) P-3(2071−2099).

4.5. Comparisons with Actual Drought Events

Figure 7 shows recently drought-affected areas. The drought in 2001 caused damage to the Han River basin as a whole, making it difficult to directly compare with Figure 7a. However, by comparing damage from 2014–2015 according to drought risk, sub-basins # 1002, # 1003, # 1011 with high DNBC-MDI overlapped actual drought-affected areas, while sub-basin # 1101 showed no drought damage and was at low risk, as shown in Figure 7b.

To analyze the relationship between the DNBC-MDI and actual drought events, an accuracy analysis was performed by determining droughts as if they were consistent with the 1994–1995, 2001, 2008–2009, 2012, and 2014–2015 droughts (shaded bars in Figure 8) and states 5 to 7 of the DNBC-MDI, as shown in Figure 8. If the DNBC-MDI matched the actual drought, a “hit” was assigned; if there was no actual drought and the DNBC-MDI was drought, then a “false alarm” was assigned; if there was a drought and the DNBC-MDI was not a drought, then a “miss” was assigned; if there was no drought and the DNBC-MDI was not a drought, then a "correct rejection" was assigned. As an accuracy measure, the production correct (PC) was calculated using Equation (5).

$$PC = \frac{a + d}{a + b + c + d} \tag{5}$$

where a, b, c, and d are the number of hits, false alarms, misses, and correct rejections, respectively.

(**a**) (**b**)

Figure 7. Drought-affected area. (**a**) 2001; (**b**) 2014–2015.

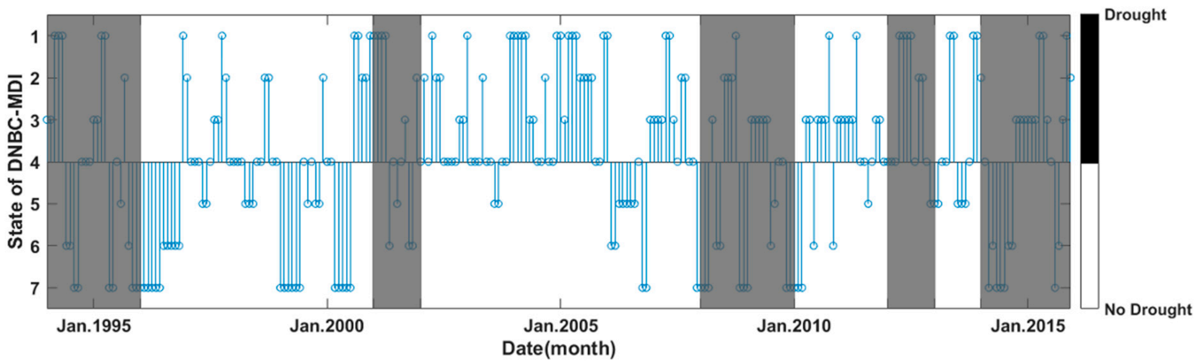

Figure 8. A comparison of actual drought events and the DNBC-MDI.

For comparative evaluation, the PC was calculated for the SPI, SDI, ESI, and DNBC-MDI. The DNBC-MDI produced the highest average PC of 0.663, followed by the SPI of 0.632, SDI of 0.639, and ESI of 0.657. Figure 9 shows the production corrections for different drought indices. The DNBC-MDI were the highest for sub-basin # 1202 (PC = 0.792) and lowest for # 1015 (PC = 0.406). The SPI had a high accuracy for sub-basin # 1302 (PC = 0.740) and showed the lowest of the accuracy for sub-basin # 1005 among the four indices. The SDI had high accuracy for sub-basin # 1303 (PC = 0.750) and with a low accuracy for # 1202 (PC = 0.542). The ESI had high accuracy for sub-basin # 1007 (PC = 0.771) and low accuracy for # 1002 (PC = 0.542).

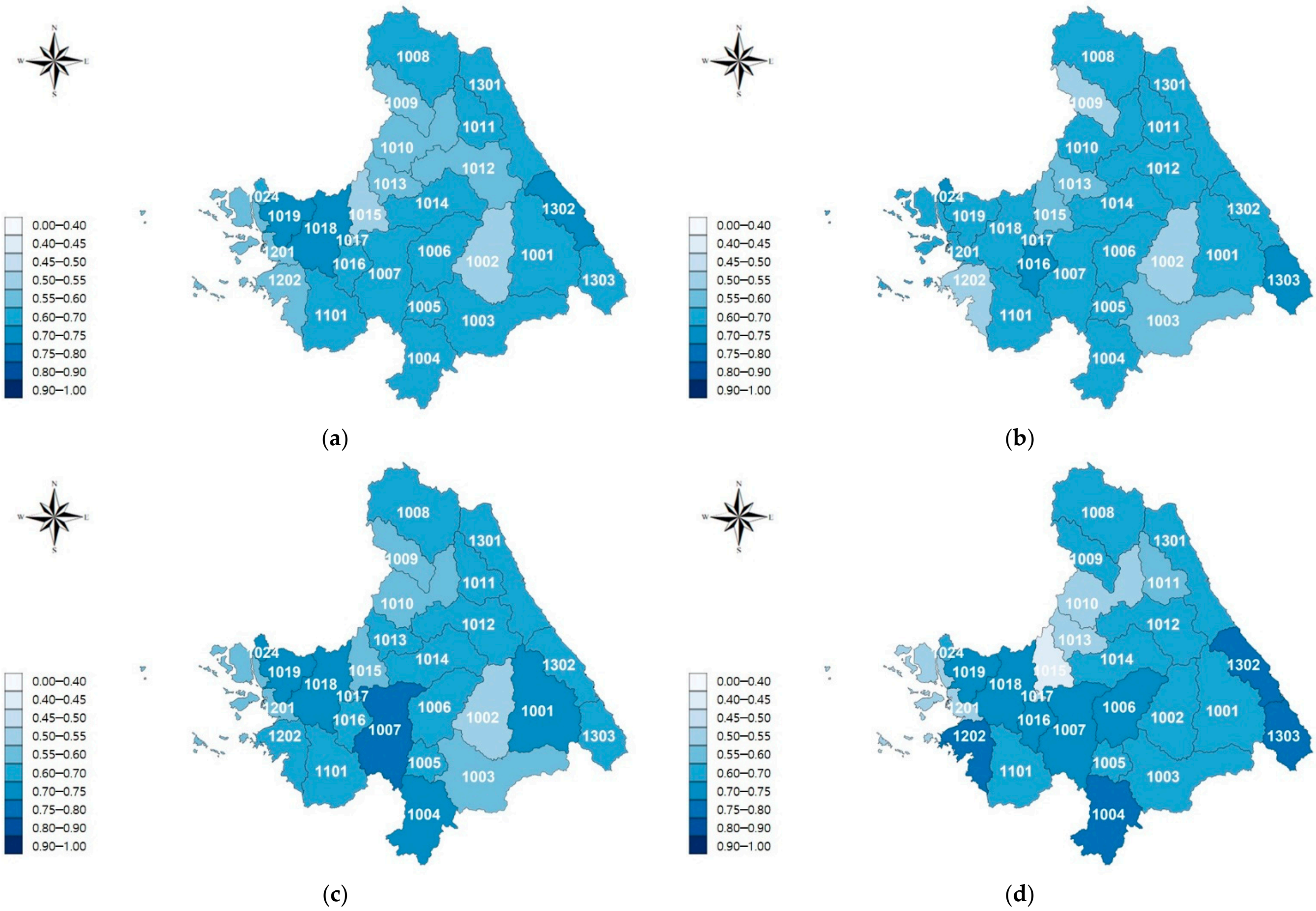

Figure 9. Production corrections for the SPI, SDI, ESI, DNBC-MDI. (**a**) SPI; (**b**) SDI; (**c**) ESI; (**d**) DNBC-MDI.

5. Conclusions

The purposes of this study were to develop a dynamic naive Bayesian classifier-based multiple-drought index (DNBC-MDI) and assess regional drought risk, taking into account various influencing factors. Especially the DNBC-MDI incorporated the drought indices and water supply capacity, which may be a key vulnerability to regional drought and useful in drought planning. Using the DNBC-MDI, a regional drought risk was comprehensively assessed for the current and future circumstances considering a climate change scenario. Based on the overall results, we concluded that the DNBC-MDI is useful in (1) combining various drought indices available for regional analysis, (2) quantifying probabilistically drought severity to detect onset and termination, and (3) applying the bivariate drought frequency analysis for comprehensive drought risk assessment.

In addition, drought assessment and drought planning are main topics in many drought-prone countries. Several systematic approaches have been suggested to develop a drought plan. For example, Knutson [32] presented six steps that attempt to reduce potential drought effects before a drought occurs when developing a country's drought plan. Among them, the second and third steps prioritize response to drought-risk areas to reduce drought damage. Wilhite [33] presented the process required for drought planning in the "10-step drought planning process", which states that vulnerability in the fourth step should be used to determine the risk of drought. Drought planning in the United States requires regional drought risks or vulnerabilities.

In this study, we aimed to develop a comprehensive drought index that could be used to develop regional drought plans. To consider various drought effects, the probabilistic droughts were evaluated incorporating SPI, SDI, and ESI, as well as the impact of droughts on water supply capacity, which is a socio-economic concern. The drought indices such as the SPI, SDI, and ESI only represent the probability of occurrence of drought but do not represent the drought vulnerability. In this study, the WSCI was used to represent the degree of vulnerability of drought, and, thus, it can be available for drought planning. For more effective monitoring of drought conditions, this study was limited to using only climate data for historic and future drought assessment. Remote sensing data of MODIS and Landsat may be useful in overcoming this weakness to quantify the hydrological extreme events and associated hazards with significant precision [34].

A growing interest in drought and the need for drought planning have led to the need for a comprehensive assessment of droughts and their risks. While the drought indices that are based on the ground and surface factors can identify drought, meteorological and hydrological factors, such as precipitation, runoff, and evaporation, can be not easily managed, but socio-economic factors can be sufficiently improved by effective management and countermeasures. Thus, it is reasonable to assess drought risks considering the socio-economic factors.

Author Contributions: Conceptualization, T.-W.K. and D.-H.P.; methodology, D.-H.P. and H.K.; validation, J.-H.A. and T.-W.K.; formal analysis, H.K.; investigation, D.-H.P.; resources, D.-H.P.; data curation, H.K.; writing—original draft preparation, D.-H.P. and H.K.; writing—review and editing, T.-W.K. and J.-H.A.; visualization, D.-H.P.; supervision, T.-W.K.; project administration, T.-W.K. All authors have read and agreed to the published version of the manuscript.

Funding: This research was supported by a grant (2020-MOIS33-006) of Lower-level and Core Disaster-Safety Technology Development Program funded by Ministry of Interior and Safety.

Institutional Review Board Statement: Not applicable.

Informed Consent Statement: Informed consent was obtained from all of the subjects involved in the study.

Data Availability Statement: Publicly available datasets were analyzed in this study. This data can be found here: (KMA website (http://www.kma.go.kr), Water Resources Management Information System (http://www.wamis.go.kr), and Asia-Pacific Economic Cooperation Climate Center (https://www.apcc21.org)).

Conflicts of Interest: The authors declare no conflict of interest.

References

1. Pachauri, R.K.; Allen, M.R.; Barros, V.R.; Broome, J.; Cramer, W.; Christ, R.; Church, J.A.; Clarke, L.; Dahe, Q.; Dasgupta, P.; et al. Climate change 2014: Synthesis report. In *Contribution of Working Groups I, II and III to the Fifth Assessment Report of the Intergovernmental Panel on Climate Change*; IPCC: Geneva, Switzerland, 2014; p. 151.
2. Sheffield, J.; Wood, E.F.; Roderick, M.L. Little change in global drought over the past 60 years. *Nature* **2012**, *491*, 435. [CrossRef] [PubMed]
3. Wilhite, D.A. *Drought Monitoring and Early Warning: Concepts, Progress and Future Challenges*; World Meteorological Organization (WMO): Geneva, Switzerland, 2006; p. 1006.
4. World Meteorological Organization (WMO). *Experts Agree on a Universal Drought Index to Cope with Climate Risks*; WMO Press Release: Geneva, Switzerland, 2009; p. 872.
5. Kim, B.S.; Chang, I.G.; Sung, J.H.; Han, H.J. Projection in future drought hazard of South Korea based on RCP climate change scenario 8.5 using SPEI. *Adv. Meteorol.* **2016**, *2016*, 4148710. [CrossRef]
6. Park, B.S.; Lee, J.H.; Kim, C.J.; Jang, H.W. Projection of future drought of Korea based on probabilistic approach using multi-model and multi climate change scenarios. *J. Korean Soc. Civ. Eng.* **2013**, *33*, 1871–1885. [CrossRef]
7. Park, M.; Lee, O.; Park, Y.; Kim, S. Future drought projection in Korea under AR5 RCP climate change scenarios. *J. Korean Soc. Hazard Mitig.* **2015**, *15*, 423–433. [CrossRef]
8. Venus, V.; Bass, S.; Brill, I.; Chinyamakobvu, E.; David, E.; Dier, S.; Frydman, I.; Hess, U.; Hori, Y.; Nyberg, J.; et al. *Drought Risk Reduction Framework and Practices*; United Nations International Strategy for Disaster Reduction Secretariat (UNISDR): Geneva, Switzerland, 2009.
9. Niemeyer, S. New drought indices. Options Mediterraneennes. *Semin. Mediterr.* **2008**, *80*, 267–274.
10. Heim, R.R. *Drought Indices: A Review. Drought: A Global Assessment*; Routledge: London, UK, 2000; pp. 159–167.
11. Heim, R.R., Jr. A review of twentieth-century drought indices used in the United States. *Bull. Am. Meteorol. Soc.* **2002**, *83*, 1149–1165. [CrossRef]

12. Vogt, J.V.; Niemeyer, S.; Somma, F.; Beaudin, I.; Viau, A.A. Drought monitoring from space. *Drought Drought Mitig. Eur.* **2000**, *14*, 167–183.
13. Ali, M.; Ghaith, M.; Wagdy, A.; Helmi, A.M. Development of a new multivariate composite drought index for the Blue Nile River Basin. *Water* **2022**, *14*, 886. [CrossRef]
14. Chen, S.; Muhammad, W.; Lee, J.H.; Kim, T.W. Assessment of probabilistic multi-index drought using a dynamic naive Bayesian classifier. *Water Resour. Manag.* **2018**, *32*, 4359–4374. [CrossRef]
15. Zargar, A.; Sadiq, R.; Naser, B.; Khan, F.I. A review of drought indices. *Environ. Rev.* **2011**, *19*, 333–349. [CrossRef]
16. Esfahanian, E.; Nejadhashemi, A.P.; Abouali, M.; Adhikari, U.; Zhang, Z.; Daneshvar, F.; Herman, M.R. Development and evaluation of a comprehensive drought index. *J. Environ. Manag.* **2017**, *185*, 31–43. [CrossRef] [PubMed]
17. Mallya, G.; Tripathi, S.; Kirshner, S.; Govindaraju, R.S. Probabilistic assessment of drought characteristics using hidden Markov model. *J. Hydrol. Eng.* **2012**, *18*, 834–845. [CrossRef]
18. Chen, S.; Shin, J.Y.; Kim, T.W. Probabilistic forecasting of drought: A hidden Markov model aggregated with the RCP 8.5 precipitation projection. *Stoch. Environ. Res. Risk Assess.* **2016**, *31*, 1061–1076. [CrossRef]
19. Palacios-Alonso, M.A.; Brizuela, C.A.; Sucar, L.E. Evolutionary learning of dynamic naive Bayesian classifiers. *J. Autom. Reason.* **2010**, *45*, 21–37. [CrossRef]
20. Shin, J.Y.; Kwon, H.H.; Lee, J.H.; Kim, T.W. Bayesian networks-based probabilistic forecasting of hydrological drought considering drought propagation. *J. Korea Water Resour. Assoc.* **2017**, *50*, 769–779.
21. Yoo, J.Y.; Kim, J.Y.; Kwon, H.H.; Kim, T.W. Sensitivity assessment of meteorological drought index using Bayesian network. *J. Korean Soc. Civ. Eng.* **2014**, *34*, 1787–1796. [CrossRef]
22. Yoo, J.Y.; Shin, J.Y.; Kim, D.; Kim, T.W. Drought risk analysis using stochastic rainfall generation model and copula functions. *J. Korea Water Resour. Assoc.* **2013**, *46*, 425–437. [CrossRef]
23. Yu, J.S.; Shin, J.Y.; Kwon, M.; Kim, T.W. Bivariate drought frequency analysis to evaluate water supply capacity of multi-purpose dam. *J. Korean Soc. Civ. Eng.* **2017**, *37*, 231–238. [CrossRef]
24. Chen, L.; Singh, V.P.; Guo, S.; Mishra, A.K.; Guo, J. Drought analysis using copulas. *J. Hydrol. Eng.* **2012**, *18*, 797–808. [CrossRef]
25. Mirabbasi, R.; Fakheri-Fard, A.; Dinpashoh, Y. Bivariate drought frequency analysis using the copula method. *Theor. Appl. Climatol.* **2012**, *108*, 191–206. [CrossRef]
26. Kim, S.; Parhi, P.; Jun, H.; Lee, J. Evaluation of drought severity with a Bayesian network analysis of multiple drought indices. *J. Water Resour. Plan. Manag.* **2017**, *144*, 05017016. [CrossRef]
27. Yu, J.S.; Yoo, J.Y.; Lee, J.H.; Kim, T.W. Estimation of drought risk through the bivariate drought frequency analysis using copula functions. *J. Korea Water Resour. Assoc.* **2016**, *49*, 217–225. [CrossRef]
28. Lee, D.R.; Moon, J.W.; Lee, D.H.; Ahn, J.H. Development of water supply capacity index to monitor droughts in a reservoir. *J. Korea Water Resour. Assoc.* **2006**, *39*, 199–214. [CrossRef]
29. Nelsen, R.B. *An Introduction to Copulas*, 2nd ed.; Springer Science & Business Media: New York, NY, USA, 2007.
30. Zhang, L.S.; Singh, V.P. Bivariate flood frequency analysis using the copula method. *J. Hydrol. Eng.* **2006**, *11*, 150–164. [CrossRef]
31. Kwak, J.W.; Kim, D.G.; Lee, J.S.; Kim, H.S. Hydrological drought analysis using copula theory. *J. Korean Soc. Civ. Eng.* **2012**, *32*, 161–168.
32. Knutson, C.; Hayes, M.; Phillips, T. *How to Reduce Drought Risk*; Western Drought Coordination Council: Lincoln, NE, USA, 1998.
33. Wilhite, D.A. Drought planning: A progress for state government. *J. Am. Water Resour. Assoc.* **1991**, *27*, 29–38. [CrossRef]
34. Memon, A.A.; Muhammad, S.; Rahman, S.; Haq, M. Flood monitoring and damage assessment using water indices: A case study of Pakistan flood-2012. *Egypt. J. Remote Sens. Space Sci.* **2015**, *18*, 99–106. [CrossRef]